8

A novel activating mutation in the kinase homology domain of natriuretic peptide receptor-2 causes extremely tall stature without skeletal deformities

Hermine A. van Duyvenvoorde,[1,2,*] Sabine E. Hannema,[1,*] Thomas Premsler,[3] Ruey-Bing Yang,[4] Thomas D. Mueller,[5] Birgit Gassner,[3] Heike Oberwinkler, [3] Ferdinand Roelfsema,[6] Gijs W.E. Santen,[2] Timothy Prickett,[7] Sarina G. Kant,[2] Annemieke J.M.H. Verkerk,[8] André G. Uitterlinden,[8] Eric Espiner,[7] Claudia A.L. Ruivenkamp,[2] Wilma Oostdijk,[1] Alberto M. Pereira,[6] Monique Losekoot, [2] Michaela Kuhn,[3,9] Jan M. Wit[1,9]

[1] Department of Pediatrics, Leiden University Medical Center, Leiden, The Netherlands

[*] These authors contributed equally

[2] Department of Clinical Genetics, Leiden University Medical Center, Leiden, The Netherlands

[3] Institute of Physiology, University of Würzburg, Germany

[4] Institute of Biomedical Sciences, Academia Sinica Taipei, Taiwan

[5] Department of Molecular Plant Physiology and Biophysics, Julius-von-Sachs-Institute, Biocenter, University of Würzburg, Germany

[6] Department of Endocrinology and Metabolic Diseases, Leiden University Medical Center, Leiden, The Netherlands

[7] Department of Medicine, University of Otago, Christchurch, New Zealand

[8] Department of Internal Medicine, Erasmus Medical Centre, Rotterdam, The Netherlands

[9] These authors jointly directed this work

Submitted

Abstract

C-type natriuretic peptide (CNP)/natriuretic peptide receptor 2 (NPR2) signalling is essential for long bone growth. In response to CNP, NPR2 synthesizes cyclic GMP, which stimulates proliferation, growth and differentiation of chondrocytes. Homozygous and compound heterozygous inactivating *NPR2* mutations cause acromesomelic dysplasia, Maroteaux type, a severe form of short-limbed dwarfism. Here we describe a novel heterozygous *NPR2* mutation (c.1963C>T, p.Arg655Cys) in an extremely tall (221 cm) male proband. CNP stimulated cyclic GMP production by the mutant NPR2 was markedly increased in skin fibroblasts of the proband as well as in transfected HEK 293 cells. Furthermore, the stimulatory effects of ATP on CNP-dependent guanylate cyclase activity were markedly enhanced, suggesting that this novel mutation enhances both the responsiveness of NPR2 to CNP and its allosteric modulation/stabilization by ATP. Coimmunoprecipitation showed that wildtype and mutant NPR2 can form stable heterodimers, suggesting a dominant positive effect. In accordance with augmented endogenous receptor activity, plasma concentration of NTproCNP (a marker of CNP production in tissues) was reduced in the proband. In summary, we report the first activating mutation within the kinase homology domain of NPR2, emphasizing the important role of this domain in the regulation of guanylate cyclase activity and bone growth by CNP.

Introduction

Natriuretic peptide receptor 2 (NPR2), also known as NPR-B or guanylate cyclase B, and encoded by the gene *NPR2*, is one of five human transmembrane receptors that catalyse the formation of cyclic GMP (cGMP) from GTP. These receptors consist of an extracellular ligand binding domain (ECD), a short membrane-spanning region and intracellularly a kinase homology domain (KHD), a helical hinge region and the C-terminal cGMP-synthesizing guanylate cyclase (GC) domain. *NPR2* is expressed by different types of cells (e.g. chondrocytes, cardiomyocytes, neurons, fibroblasts and vascular smooth muscle cells), in different tissues (e.g. in bone, brain, heart, vasculature, lung, ovary) [1]. Its ligand is C-type natriuretic peptide (CNP), a paracrine hormone of the natriuretic peptide family. In the absence of CNP, NPR2 exists as a homodimer or homotetramer, and ligand binding does not lead to further aggregation [1, 2]. Multiple extra- and intracellular domains mediate this oligomerization. The intracellular oligomerization interface region has been mapped to the amphipathic sequence that bisects the KHD and GC domains [1]. Based on structural studies of the homologous protein NPR1 (also known as NPR-A or guanlyate cylcase A, the receptor for atrial natriuretic peptide (ANP), which exhibits 78% sequence identity to NPR2 [3]) it is postulated that CNP-induced rotation of the ECD is transmitted across the membrane and reorients the two intracellular domains into the active conformation, thereby enabling cGMP synthesis.

Studies in genetic mouse models revealed that CNP-NPR2-cGMP signalling is essential for stimulation of endochondral ossification required for long bone growth, for oocyte maturation and for sensory axon bifurcation in the spinal cord [4-6]. In humans, homozygous and compound heterozygous inactivating *NPR2* mutations cause acromesomelic dysplasia, Maroteaux type (AMDM) [7], and heterozygous inactivating mutations have been associated with short stature [8]. Enhanced production of CNP caused by chromosomal translocations results in tall stature, a Marfanoid phenotype and skeletal abnormalities [9,10]. Concordantly, an activating *NPR2* mutation located in the GC domain also causes skeletal overgrowth [11].

Here we describe a novel heterozygous activating *NPR2* mutation located within the KHD, in a proband with extremely tall stature but with only mild skeletal deformities. We show an increased cGMP response of the mutant NPR2 to CNP in the proband's skin fibroblasts and in transfected HEK 293 cells, and suppressed markers of tissue CNP production in the proband's serum, in accordance with increased NPR2 activity *in vivo*.

Materials and methods

GH and prolactin secretion studies

The healthy volunteers of the present study participated in previous studies on pituitary hormone secretory dynamics; testing conditions were previously described [12, 13]. Blood samples (2.0 ml) were withdrawn at 10-min intervals for 24 h, and stored at -20°C for hormone measurements. Plasma GH concentrations were measured with a sensitive time-resolved fluoroimmunoassay (Wallac, Turku, Finland). The assay is specific for 22-kDa GH and was previously described in detail [14]. Plasma prolactin concentrations were measured with a sensitive time-resolved fluoroimmunoassay (Wallac Oy, Turku, Finland), details were previously described [13]. Hormone concentration time series were analyzed via a recently developed automated deconvolution method, empirically validated using hypothalamo-pituitary sampling and simulated pulsatile time series [15, 16].

DNA analysis

Genomic DNA was isolated from peripheral blood samples using the AUTOPURE LS Instrument (Gentra Systems). Cytogenetic microarray analysis was performed using the Affymetrix CytoScan HD Array according to the manufacturer's procedures. Copy number was assessed in the proband using ChAS software (Chromosome Analysis Suite) (Affymetrix, California, USA). Whole exome sequencing was performed on DNA fragmented into 200-400 bp fragments using Covaris Adaptive Focused Acoustics (AFA) shearing according to the manufacturer's instructions (Covaris, Inc., Woburn, MA). The exome was captured by Nimblegen SeqCap EZ V2 kit (Roche Nimblegen, Inc., Madison, WI) in combination with Illumina paired end library preparation and 2x 100 bp sequencing with at least 70x mean coverage. Downstream analyses included demultiplexing (CASAVA software, Illumina), sequence quality control, capture quality control, SNP calling and indel (insertions and deletions) calling using different software applications as described by Santen et al [17]. The *NPR2* mutation was confirmed by Sanger sequencing using standard procedures (primer sequences available on request).

Site-directed mutagenesis and intracellular cGMP responses of transfected HEK 293 cells

The expression plasmid encoding a FLAG-tagged NPR2 Arg655Cys mutant protein was generated by PCR-mediated mutagenesis using FLAG-tagged NPR2 in pFLAG-CMV1 [18]. Two oligonucleotides were synthesized; Arg655Cys-forward: 5'- cc aac tgt gtg gtg gat agt tgc ttt gtg ctc aaa ata aca g -3' and Arg655Cys-reverse: 5'- ct gtt att ttg agc aca aag caa cta tcc acc aca cag ttg g -3' (the underlined nucleotides represent the site of Arg655Cys mutation), to change residue arginine$_{655}$ to cysteine. Mutagenesis was performed using a Quick-Change site-directed mutagenesis kit (Agilent Technologies). The mutation and the absence

of unwanted mutations were verified by sequencing. HEK 293 cells were transiently transfected with the FLAG- or Myc-tagged wildtype or mutant NPR2 expression constructs using FuGene (Roche). Transfected cells were serum-starved for 4 h prior to CNP exposure (48 h after transfection). Cells were pretreated with 0.1 mM of the phosphodiesterase inhibitor 3-isobutyl-1-methylxanthine (IBMX) for 15 min, and then exposed to various concentrations of CNP (Bachem, Heidelberg, Germany) for another 10 min. Intracellular cGMP contents were determined by radioimmunoassay [19, 20].

Guanylate cyclase assays

GC activity of crude membranes prepared from transfected HEK 293 cells was essentially assessed as described before [19]. Activity assays were carried out in 50 mM HEPES buffer, pH 7.4, containing 50 mM NaCl, 5% glycerol, 0.05% BSA, 1 mM IBMX, 2 mM GTP, 30 mM creatine phosphate, 1.5 U/ml creatine phosphokinase, and different concentrations of ATP (as indicated in the results section) [19]. To stimulate GC activity, membranes (20 µg protein) were incubated with 0.01 to 1000 nM CNP (ligand dependent activity), or with 1% (v/v) Triton X-100 (detergent stimulated, maximal activity) during 10 min [19]. cGMP formation was measured by radioimmunoassay [19, 20]. The basal and CNP-stimulated cGMP responses were calculated as percentage of the maximal, Triton-stimulated activity. NPR2 expression levels in the cytosol versus membrane fractions were assessed by Western blotting using an antibody against the FLAG epitope (Cell Signaling).

Isolation and culture of human skin fibroblasts and cGMP determinations

Skin biopsies were taken from the proband and a control donor, and a culture of dermal fibroblasts was established as previously described [21]. Experiments were performed with cells with a passage number ranging between 5 and 7 in mitogen-free, serum-reduced DMEM (0.5% fetal calf serum during 3 h prior to experimentation). Cells were pretreated with 0.1 mM IBMX for 15 min, and then exposed to CNP (0.1-1000 nM) for another 10 min. Intracellular cGMP contents were determined by RIA [19, 20].

Coimmunoprecipitation and Western blot analyses

For co-expression of FLAG-tagged wildtype NPR2 and Myc-tagged mutant NPR2, the FLAG (DYKDDDDK) and Myc (EQKLISEEDL) epitopes were positioned directly after the cleavage site of the NPR2 signal peptide by PCR-mediated mutagenesis. HEK 293 cells were prepared in 10 cm dishes and (co)transfected with 10 µg plasmid as described above. After 48 h cells were lysed at 4°C for 30 min in 250 µl of lysis buffer (20 mM Tris-HCl, 150 mM NaCl, 1 mM Na_2EDTA, 1 mM EGTA, 1% Triton X-100, pH 7.5), with protease and phosphatase inhibitors (Roche). After centrifugation (2000 g, 10 min, 4°C), the supernatant was incubated with 25

µl pre-equilibrated anti-FLAG M2 affinity gel beads (Sigma) at 4°C for 2 h. The beads were washed three times, resuspended in 100 µl of electrophoresis sample buffer (200 mM Tris·HCl, pH 6.8, 6% (w/v) SDS, 15% glycerol, 10% ß-mercaptoethanol, 0.01% bromophenol blue) and boiled for 10 min. For Western blot analyses, protein samples were resolved by 10% SDS-PAGE. Electrophoresis and immunoblotting were performed as previously described [20]. Antibodies were anti-FLAG (Cell Signaling) or anti-Myc (Bioscience).

Modeling of the NPR2 mutant Arg655Cys

The full-length model of NPR2 was built from homology models of the individual domains on the basis of structure templates for the NPR2 ECD (protein data bank (PDB) entries 1DP4, 1T34, crystal structure of free and ligand-bound NPR1), the KHD (2EVA, 3P86, 2PHK) and the GC domain (3ET6). Since no structural templates are available for the linker regions, secondary structure prediction was applied using the amino acid sequence. A *de novo* modeling approach was applied to connect the individually modeled domains, ECD, KHD and GC. As the structure of the linker domains is purely speculative, the full-length model serves only representative purposes and was not used to predict or propose any activation mechanism. The most suited templates for modeling of the individual domains were identified by Basic Local Alignment Search Tool (BLAST) searches using the amino acid sequence of the individual domains (KHD and GC) and the PDB (http://www.rcsb.org). For modeling of the KHD, the best match of the BLAST search (PDB entry 3P86, crystal structure of the Crt1 kinase, a member of the raf-like kinase family, [22]) was used to obtain a 3D model. In addition, to minimize model bias, structures of kinases with lower E-values and amino acid sequence identity (i.e. PDB entries 2EVA: Kinase TAK1, a member of the MAPKKK family [23], and 2PHK: Phosphorylase kinase-γt [24]) were also used to build models for the KHD of NPR2. The model for the GC domain of NPR2 was obtained using the crystal structure of a soluble eukaryotic guanylyl cyclase, which was shown to exist as homodimer and is specific for cGMP (PDB entry 3ET6). The models were obtained either from automatic modeling using the SWISS-MODEL server [25] providing a sequence alignment and the structure template or by manually exchanging residues of the structure template using a multiple sequence alignment of target and template sequences using the software Quanta2008 (MSI Accelrys). Deletion and insertions between target and template molecule were modeled by manual model building. Sequence alignments were made using the software CLUSTALW.

CNP, ANP and BNP Assays

Plasma ANP, BNP, CNP and NTproCNP, following extraction over C18 SepPac cartridges (Waters Corp., Milford, MA), were measured by RIA as previously described [26, 27]. Recoveries

for CNP22 and NTproCNP over SepPac cartridges were 98% and 108% respectively. Crossreactivity of human BNP (at 100 pmol/L) in the CNP assay is approximately 4%. CNP concentrations were not corrected for BNP crossreactivity. Crossreactivity of CNP and human BNP in the NTproCNP assay was <0.05% for both.

Data Analysis

Statistical comparisons were done using Student's t test ($p < 0.05$). Data are given as mean ± S.E.

Results

Case - clinical description and investigations

Growth and skeletal phenotype. The proband was born at term with a weight of 4 kg (+ 1 standard deviation score (SDS)) and a length of 62 cm (+ 6 SDS). He continued to be tall in infancy, childhood and adolescence. Psychomotor development was normal but puberty started late, at the age of approximately 15 yr. At age 16 yr his height was 216 cm; on X-ray his epiphyses were 'wide open' but the exact bone age was not documented. He underwent epiphysiodesis of the distal femur and proximal tibia and fibula. His adult height is 221 cm (+ 5.2 SDS), sitting height is 107.8 cm (+3.7 SDS), sitting height/height ratio 0.49 (-1.3 SDS), arm span 232 cm, weight 155 kg, and head circumference 60 cm (+1.2 SDS) (Figure 1A). He has suffered several fractures, mainly due to sports accidents, and one metatarsal fracture after a long hike. Physical examination showed long fingers and mild thoracic kyphosis (Figures 1B and C). He did not have particularly long halluces (Figure 1D) or a Marfanoid habitus, which were described in the previously reported cases with increased CNP production or an activating *NPR2* mutation [9-11]. A skeletal survey demonstrated mild scoliosis and secondary degenerative changes of the skeleton, coxa valga with slightly flat femoral heads and mild right hip dysplasia (Figures 1E-I). Bone mineral density was normal (Z-score lumbar spine +1.9, hips +1.6 and +1.4, as determined by dexa scan (Hologic Discovery A)).

Cardiovascular system. Chronic venous insufficiency of the lower extremities was present since the age of 36 yr. Blood pressure was 130/80 mmHg, with a regular pulse. Echocardiography showed normal cardiac size (corrected for BMI) and contractile functions, with the exception of paroxysmal atrial fibrillation.

Endocrinology. Non-insulin dependent diabetes mellitus (NIDDM) was diagnosed at age 53 yr and is well controlled with metformin. Testicular volumes were normal, with a cystic abnormality of 4 mm in the left testis and a solitary microcalcification in the right testis on ultrasound.

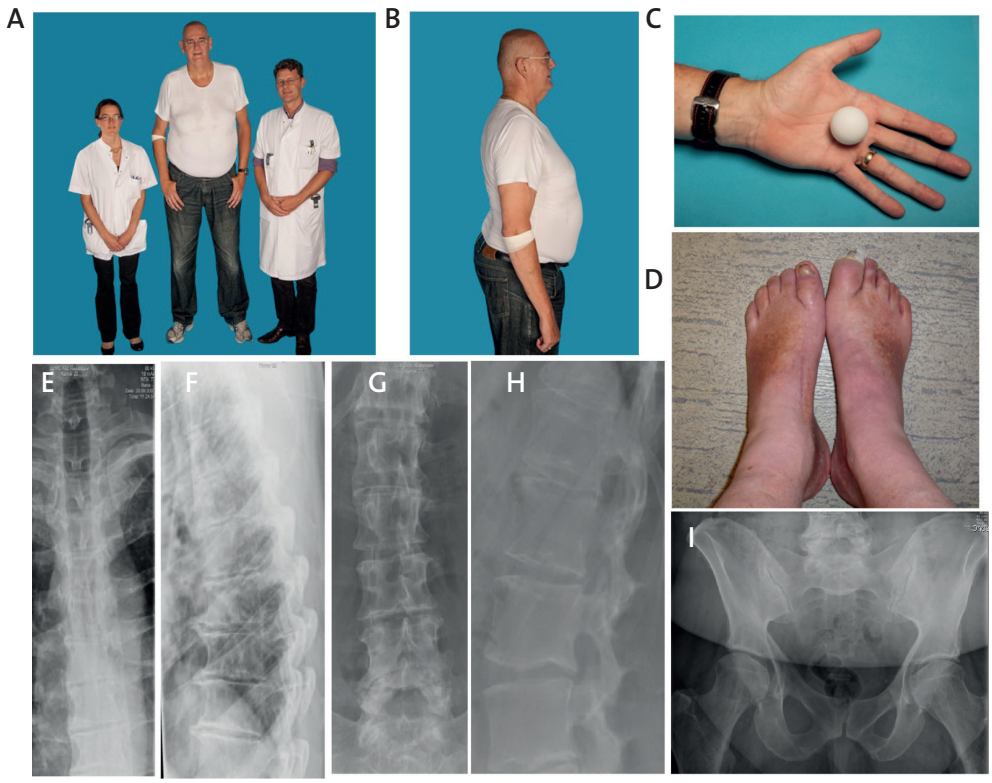

Figure 1 Clinical features of the proband

(A-D) Photographs of the proband, showing no Marfanoid habitus. **(A)** Proband with two of the authors (SEH, 173 cm, AMP, 192 cm). **(B)** Lateral photograph showing increased thoracic kyphosis and lumbar lordosis. **(C)** Proband's hand, holding a ping-pong ball for reference, showing long fingers. **(D)** Proband's feet, halluces are not particularly long. **(EF)** Posterioanterior and lateral radiographs of the thoracic spine. (GH) Posterioanterior and lateral radiographs of the lumbar spine, showing mild scoliosis. **(I)** Pelvic radiograph showing coxa valga, slightly flat femoral heads, mild right hip dysplasia and degenerative changes. The proband gave permission for publication of these photographs.

He has bilateral gynaecomastia and serum prolactin was elevated on two occasions. At age 55 yr the 24 h growth hormone (GH) and prolactin secretion rates were quantified showing low-normal GH secretion compared to control subjects (nine healthy males aged 47-61 yr, BMI 21-31 kg/m^2) (Supplemental figure 1A). Both basal and pulsatile prolactin secretion, however, were markedly increased with a total secretion of 679 µg/l distribution volume per 24 h compared to 183 µg/l distribution volume per 24 h (range 99-325) in the controls (Supplemental figure 1B and Table 1 of supplemental data). The only medication used at the time of sampling was lactulose (to treat constipation), which is not known to alter prolactin secretion. Although a recent prolactin level, at age 61 yr, was within the normal range (Table 1), this does not necessarily indicate that prolactin secretion has normalised since the serum levels were not constantly elevated during the 24 h profile either. Levels of other relevant hormones were in the normal range (Table 1).
Neurology. Axonal sensorimotor polyneuropathy was diagnosed at age 41 yr and was later attributed to NIDDM.

Identification of *NPR2* mutation and microdeletion on chromosome 15q

Because the tall stature was not due to GH overproduction and the proband did not show features of any known syndrome, a SNP array analysis was performed. This showed a heterozygous microdeletion in chromosome 15 (karyotype: array 15q25.2q25.3(85,084,470-85,724,984)x1 (Human Genome 19)), containing 8 genes (*ZSCAN2*, *WDR73*, *NMB*, *SEC11A*, *ZNF592*, *ALPK3*, *SLC28A1* and *PDE8A),* encoding the following proteins: zinc finger and SCAN domain-containing protein 2, WD repeat-containing protein 73, neuromedin-B, signal peptidase complex catalytic subunit SEC11A, zinc finger protein 592, alpha-kinase 3, sodium/nucleoside cotransporter 1 and cAMP-specific phosphodiesterase 8A, respectively). Sequencing of this region on the remaining allele showed no mutations. Since this microdeletion cannot explain the tall stature, we subsequently performed whole exome sequencing and identified a heterozygous c.1963C>T mutation in the *NPR2* gene, predicted to exchange arginine at position 655 to cysteine within the KHD of NPR2. The mutation and microdeletion were not found in the proband's sister or son, who are not as tall as the proband (Figure 2). Unfortunately, we were unable to investigate other family members.

Site-directed mutagenesis shows that the substitution Arg655Cys enhances the guanylate cyclase activity of NPR2

We tested the function of the mutant $NPR2_{Arg655Cys}$ by transfecting HEK 293 cells and measuring cGMP production under baseline conditions and after stimulation with CNP.

Table 1 Blood biochemistry tests

Parameter	Age 55 yr	Age 61 yr	Unit	Normal range
Urea		10.7	mmol/l	2.5-7.5
Creatinin	58	70	µmol/l	64-104
SGOT	35	38	U/l	0-35
SGPT	32	52	U/l	0-45
Calcium	2.25	2.46	mmol/l	2.15-2.55
Phosphate	0.83	0.88	mmol/l	0.9-1.5
Alkaline phosphatase	79	87	U/l	0-115
P1NP	36		ng/ml	<59
Beta crosslaps		0.17	ng/ml	<0.704
HbA1c	6.3		%	4.3-6.3
HbA1c		45	mmol/mmol Hb	20-42
Cholesterol	5.19	4.86	mmol/l	3.9-7.3
Triglycerides	1.88	1.03	mmol/l	0.8-2.3
TSH	2.96	1.99	mU/l	0.3-4.8
FT4	14.3	15.5	pmol/l	10-24
IGF-I	15.3 (+0.5 SDS)	28.5 (+3.1 SDS)	nmol/l	7-83
IGFBP-3	1.6	3.8	mg/l	1.5-6
Prolactin	17.1	8.1	µg/l	4-15
Cortisol (8:00)	0.422		µmol/l	0.1-0.6
Androstenedione	4.1	1.7	nmol/l	2-10
DHEA-S	3.09	1.7	µmol/l	2-15
FSH	4.1	6.9	U/l	2-10
LH	3.2	4.6	U/l	2-9
Testosterone	9.1	13	nmol/l	8-31
Estradiol		71	pmol/l	70-200
Estrone		227	pmol/l	100-200
AMH		1.6	µg/l	5.1-9.1
Inhibin B		112	ng/l	150-400
ANP		32.8	pmol/l	4-27
BNP		7.8	pmol/l	3-12
CNP		0.9	pmol/l	0.5-1.2
NTproCNP		8.1	pmol/l	12-25
cGMP		5.8	nmol/l	2.5-7.7

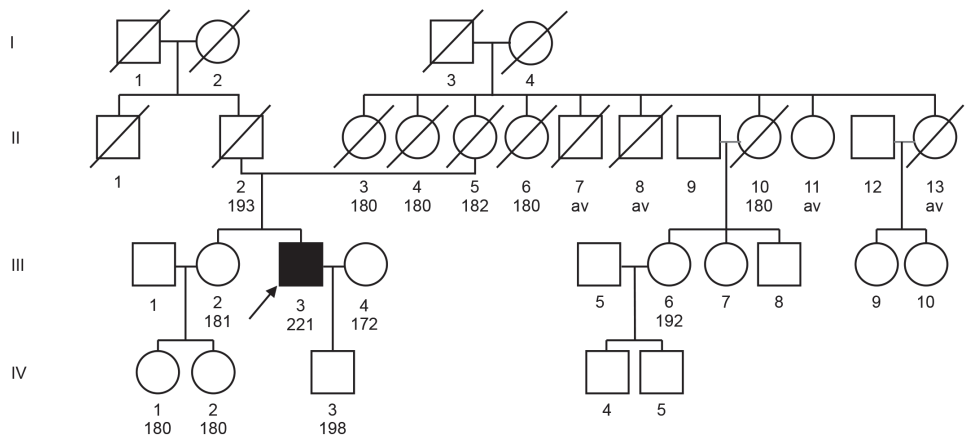

Figure 2 Family pedigree

The proband, III-3, is indicated with an arrow. The *NPR2* mutation and microdeletion on chromosome 15 were absent in his sister and son, other family members have not been investigated. Heights of family members (in cm), as reported by the proband, are indicated below the symbols. Heart valve pathology is indicated with hatching. Av = average height.

Transfection with cDNA encoding the FLAG-tagged mutant NPR2 produced equivalent amounts of membrane protein, compared with FLAG-tagged wildtype NPR2, suggesting that the mutation does not alter protein synthesis and membrane localization (see Western blots depicted in Figures 3A and B). However, basal cGMP contents of cells expressing mutant NPR2 were ~2.1 ± 0.3-fold higher in comparison with cells expressing wildtype NPR2 (n = 3). Intracellular cGMP levels were increased by CNP in a concentration-dependent manner, and these responses were much greater in cells expressing the mutant protein as compared to cells expressing wildtype NPR2 (Figure 3A). Intriguingly, co-expression of wildtype and mutant NPR2 resulted in cGMP responses to CNP which were almost as high as those observed with mutant NPR2 alone (Figure 3A).

Additionally, the effect of this amino acid substitution on NPR2 activity was evaluated in guanylate cyclase assays performed with crude membranes from transfected HEK 293 cells expressing either the wildtype or the mutated receptor, or both (Figure 3B). The membranes were incubated with CNP, and cGMP formation was measured by RIA [19]. Assays were performed in the presence of 2 mM ATP to mimic cytoplasmic ATP levels, which are in the range of 1-10 mM [28]. Again we confirmed, by immunoblotting, that mutant and wildtype FLAG-tagged NPR2, and their combination, were expressed in similar amounts (see inset

of Figure 3B). In addition, to account for small differences in the expression level of the two variants, we normalized the CNP-stimulated activity data to the respective maximal, Triton-stimulated NPR2 activity [19]. Wildtype NPR2 responded to CNP with a concentration-dependent increase in cGMP production (Figure 3B). In comparison, CNP-stimulated cGMP production by membranes containing mutant NPR2 or both mutant and wildtype NPR2 was markedly enhanced (Figure 3B).

Wildtype NPR2 can form heterodimers with mutant NPR2

Although the NPR2 contains a single cyclase catalytic site per polypeptide chain, a dimeric receptor assembly is essential for the activation of the catalytic domain [1]. The introduction of the Arg655Cys mutation in individual subunits could therefore lead to the formation of hyperfunctional dimers. The observation that co-expression of wildtype and mutant NPR2 resulted in cGMP responses to CNP close to those observed with mutant NPR2 alone suggested this "dominant positive" effect. Indeed, co-immunoprecipitation of FLAG-tagged wildtype NPR2 and Myc-tagged mutant NPR2 confirmed a tight interaction of both proteins (Figure 3C).

Arg655Cys substitution results in increased activity of native NPR2 in skin fibroblasts

To study the mutant NPR2 in primary cells we used cultured fibroblasts harvested and expanded from a skin biopsy from the proband's forearm. Intracellular cGMP levels were compared to levels in control skin fibroblasts obtained from a healthy 48 yr-old male donor with a height of 192 cm. Basal cGMP contents were similar in proband and control fibroblasts but the responses to CNP were markedly increased in the former (Figure 4A). In contrast, the cGMP responses to ANP, which are mediated by NPR1, were not different between proband and control fibroblasts (Figure 4B). This confirms increased CNP-stimulated activity of the mutant NPR2 not only when transfected into HEK 293 cells but also when naturally expressed in fibroblasts.

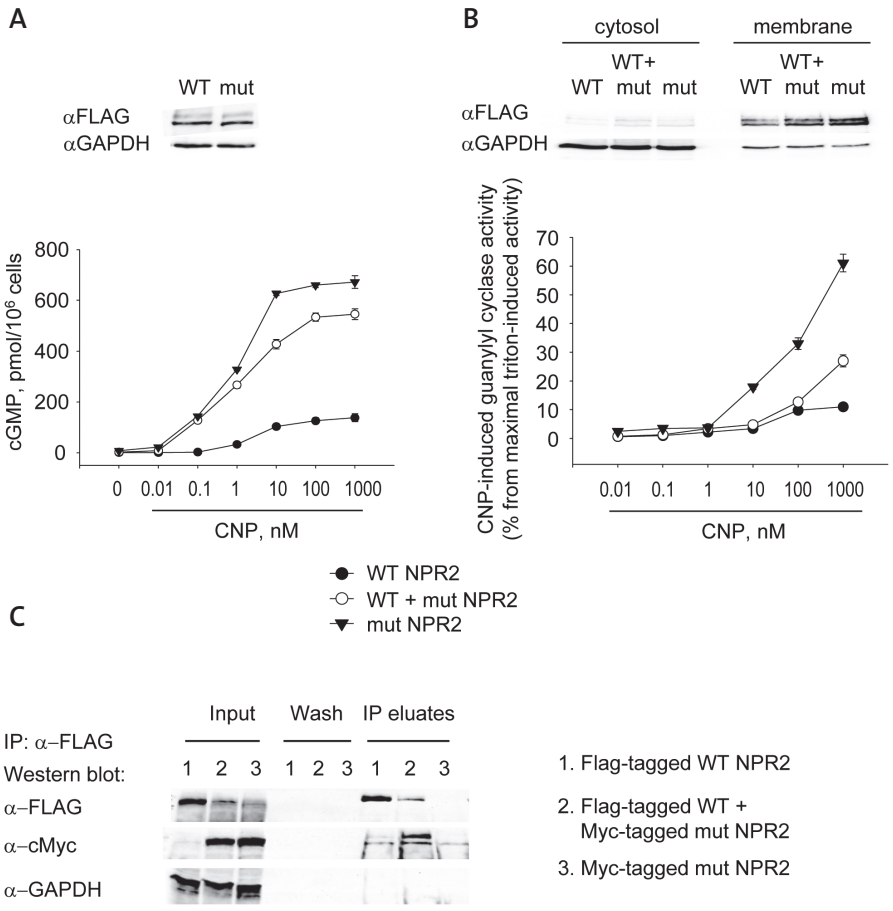

Figure 3 Increased cGMP responses to CNP of HEK 293 cells expressing mutant NPR2
(A) HEK 293 cells expressing FLAG-tagged wildtype (WT) or mutant (mut) NPR2, or both, were incubated with CNP (10 pM – 1 mM, 10 min). Whole cell cGMP contents were quantified by RIA (n=3 per condition). **(B)** Crude membranes prepared from HEK 293 cells expressing FLAG-tagged wildtype (WT) NPR2, mutant NPR2 (mut), or both, were incubated with vehicle, CNP or detergent (1% Triton X-100). cGMP production was measured by RIA in [fmol cGMP·(µg protein)–1·min–1]. All values were calculated as *X*-fold of the maximal Triton-induced activity (n=4 per condition). *Insets in A,B*: Western blots demonstrating similar expression levels of WT and mutated NPR2 in transfected HEK 293 cells (all 50 µg protein per lane). **(C)** Heterodimer formation of wildtype and mutant NPR2. Extracts from cells transfected with FLAG-NPR2 and pCMV5 (Mock), cells with FLAG-NPR2 and Myc-tagged mutant-NPR2, or cells with pCMV5 and Myc-tagged mutant NPR2 were immunoprecipitated (IP) with anti (α)-FLAG M2 affinity gel beads (Sigma). Aliquots of cell lysates (before IP: input) as well as the IP proteins were analyzed by Western blot and subsequent FLAG- and Myc-specific immunodetection. Results show that Myc-tagged mutant NRP2 is precipitated with FLAG-tagged wildtype NPR2, indicating interaction between these two isoforms. Similar data were obtained in two independent experiments.

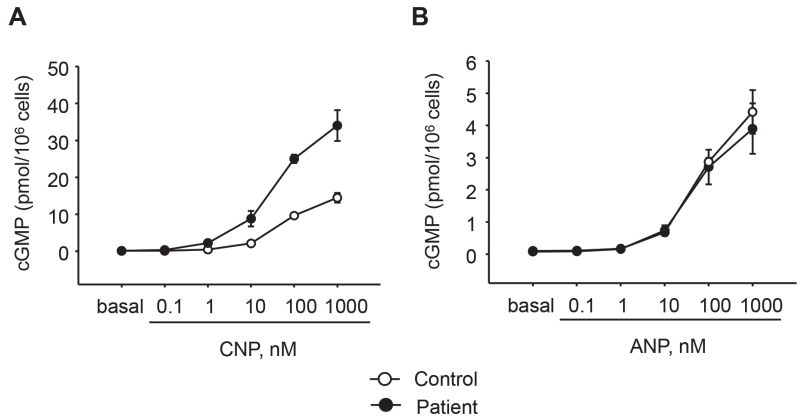

Figure 4 Increased effects of CNP on cGMP levels of proband´s skin fibroblasts
Proband and control fibroblasts were incubated with vehicle, CNP or ANP (both 0.1 nM – 1 mM) for 10 min, and intracellular cGMP contents were determined by RIA (n=8). (**A**) In comparison to the control fibroblasts, the CNP-induced cGMP-responses of the proband's fibroblasts were markedly increased. (**B**) The responses to ANP remained unaltered.

Homology modeling studies

As mentioned above, in contrast to previously published mutations directly affecting the GC domain, the novel mutation that we describe here is localized within the KHD of NPR2. Although the KHD binds ATP [29], kinase activity has never been demonstrated [30]. Modeling indeed revealed that although all elements required for ATP binding are present [31], the lack of kinase activity is likely linked to the loss of the conserved aspartate in the activation loop which is replaced by a serine (Ser644) in NPR. This abstracts the proton from the phospho-group acceptor required for the γ-phosphate transfer from ATP [32]. However, experiments by Duda *et al*. have shown that ATP binding to the KHD is coupled to a conformational rearrangement which possibly results in allosteric modulation of the GC domain [31].

To obtain insights into the molecular mechanism by which the Arg655Cys substitution influences NPR2 activation, we performed homology modeling to derive 3D models of the different protein domains (Figure 5). First a model of the mutation-carrying KHD was prepared (Figure 5A). Several different structure templates of protein kinases from the protein structure data bank RCSB were used to minimize structural bias of the KHD model towards a particular kinase template. In all models prepared, residue Arg655 is located at the solvent-accessible surface of the KHD (Figure 5B and C). The residue shares no direct contact with the ATP binding pocket or the dynamic linker connecting the upper and lower lobe of the kinase (Figure 5B and C). Thus, our modeling study suggests that the mutation does not directly influence ATP binding. Furthermore, an influence of the mutation Arg→Cys on protein folding seems unlikely due to the solvent-exposed position of Arg655.

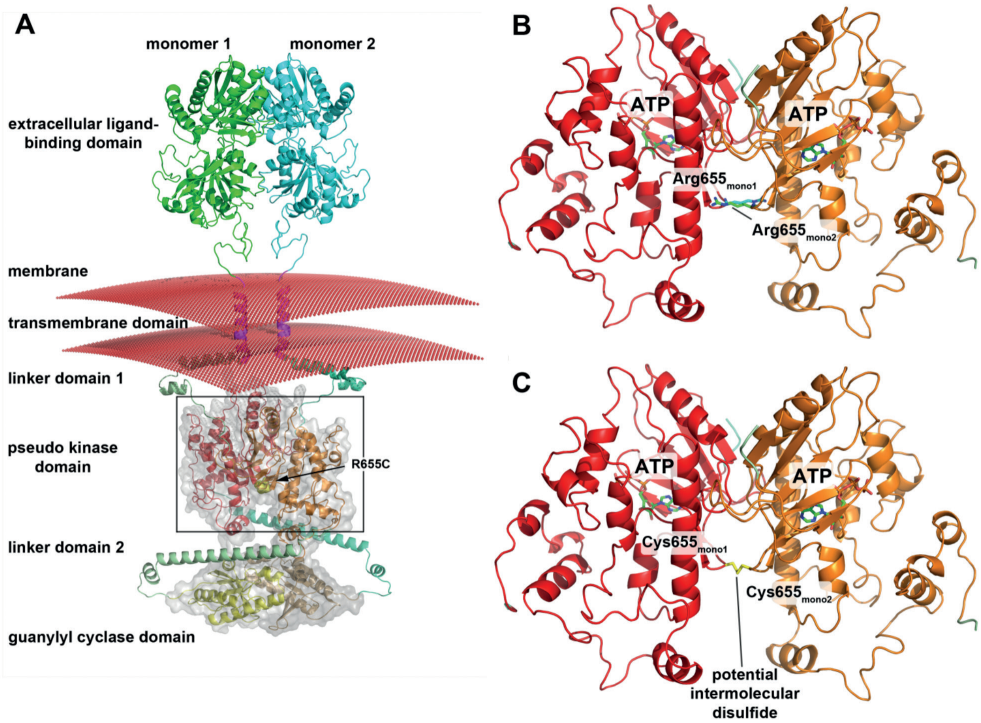

Figure 5 Homology modeling

(**A**) A theoretical model of NPR2 consisting of the ECD connected to the KHD and GC domains via a single transmembrane domain. The structurally characterized domains were modeled on the basis of structure templates obtained from the PDB databank, the linker regions were built on the basis of secondary structure predictions. Thus the full-length model only serves illustrative purposes. The area within the rectangle is shown in more detail in figures B and C. (**B**) A 3D model of the KHD of wildtype NPR2. The dimer assembly was obtained by docking the monomeric model structure of KHD onto the kinase structure of Crt1 (PDB entry 3P86). The side chain of arginine at position 655 (indicated as sticks) is located close to the dimer interface thereby possibly restraining the conformational rearrangement of the dimer assembly due to steric and electrostatic forces. (**C**) Replacement of the bulky, positively charged arginine side chain by a small and neutral cysteine could potentially relieve these restraints. Alternatively, the close proximity of two Cys655 residues in a homodimeric NPR2 mutant assembly might allow the formation of an intermolecular disulfide bridge leading to a semiactivated receptor.

Arg655Cys substitution enhances the ATP-dependent activation of NPR2

To test whether the mutation of Arg655 to cysteine influences the modulatory effect of ATP on cyclase activity, we performed CNP concentration-response assays in the absence and presence of three different concentrations of ATP (10, 100 and 1000 nM). NPR2 activity was evaluated in guanylate cyclase assays performed with crude membranes prepared from transfected HEK 293 cells. Again we confirmed that mutant and wildtype FLAG-tagged NPR2 receptors were expressed in similar amounts (see Figure 6, upper part) and we normalized the CNP-stimulated activity to the maximal, Triton-stimulated NPR2 activity [19]. In the absence of ATP, the cGMP-responses of wildtype NPR2 to CNP were small: 1.1-fold (in response to 1 nM CNP), 2-fold (10 nM CNP) and 6-fold (100 nM CNP) increases of baseline activity. Basal and CNP-stimulated activities of mutant NPR2 were only slightly enhanced. More precisely, baseline activity of mutant NPR2 was 2-fold higher as compared to wildtype NPR2. In response to CNP baseline cGMP production raised 3-fold (1 nM CNP), 4.6-fold (10 nM CNP) and 6-fold (100 nM CNP) (n=4 per condition). In the absence of CNP, ATP (10-1000 nM) barely influenced cyclase activities of the wildtype and mutant receptors (Figure 6). However, increasing concentrations of ATP enhanced the ligand-dependent activation of wildtype and mutant NPR2. Notably, ATP increased the potency of CNP much more for the mutant as compared to the wildtype receptor (Figure 6).

Decreased level of NT-proCNP in proband's plasma

To assess whether increased NPR2 activity *in vivo* leads to reduced production of its ligand we measured the proband´s plasma levels of the CNP prohormone (NTproCNP) and the processed peptide (CNP) by respective radioimmunoassays. When renal function is normal, plasma NTproCNP level is a better reflection of CNP production in tissues than plasma CNP [33, 34]. While the concentration of NTproCNP was diminished (8.1 pmol/l, which is 3.3 SD below the mean for a subject of his age and sex; normal range in healthy donors of the same age: 12-25.0 pmol/l [34]), the plasma CNP concentration was normal (0.9 pmol/l; reference range 0.5-1.2 pmol/l). Plasma cGMP concentration in the same sample was within normal limits (5.8 nmol/l, normal range 2.5-7.7 nmol/l). Plasma ANP was mildly elevated (32.8 pmol/l, normal 4-27) and brain natriuretic peptide (BNP) level was 7.8 pmol/l (normal 3-12 pmol/l).

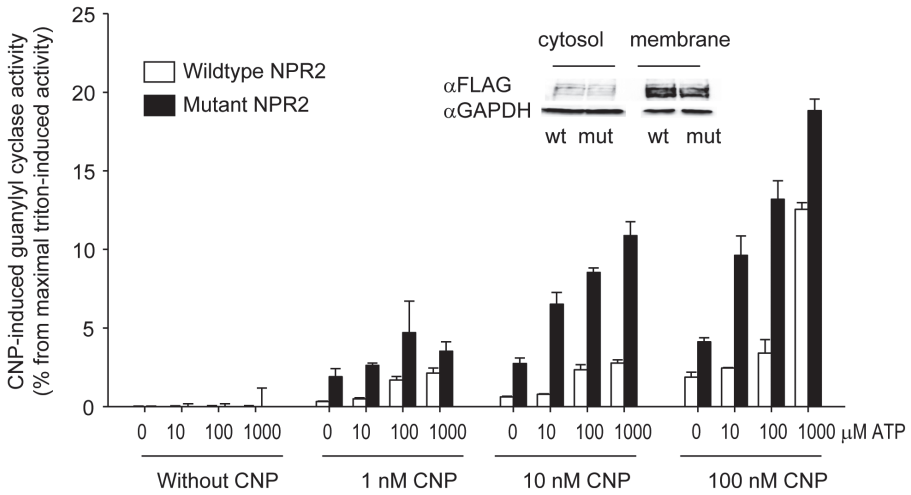

Figure 6 Enhanced modulatory effect of ATP on CNP-dependent guanylyl cyclase activity of mutant NPR2

GC activity was determined in crude membranes prepared from HEK 293 cells (expressing wildtype or mutant NPR2) in the absence or presence of ATP (10-1000 nM) and the indicated concentrations of CNP (n=4). *Inset:* Western blots demonstrating similar membrane location and expression of WT and mutated NPR2 in transfected HEK 293 cells (all 50 μg protein per lane).

Discussion

We identified a novel heterozygous *NPR2* mutation in a proband with extremely tall stature. *In vitro* assays with transfected HEK 293 cells showed that the NPR2 variant Arg655Cys can form stable heterodimers with the wildtype receptor and responds to CNP with markedly enhanced cGMP production. *Ex vivo* studies with the proband's fibroblasts confirmed that the endogenously expressed NPR2 variant mediates markedly enhanced CNP/cGMP signalling. Because this pathway is critically involved in bone development by stimulating growth plate chondrocyte differentiation and proliferation [4] and an activating *NPR2* mutation was previously found to result in tall stature [11], we conclude that the Arg655Cys mutation is responsible for the observed skeletal overgrowth in the proband.

Reduced production of CNP, as reflected by low NTproCNP level in the proband's plasma, is consistent with increased NPR2 activity *in vivo*. Low NTproCNP levels were also reported in two of the three Japanese patients with an activating mutation in the GC domain of

NPR2 [11] and are opposite to the marked increase in plasma CNP levels in subjects with loss of function mutations in *NPR2* [8, 34]. Together, these findings suggest the presence of a negative feedback mechanism whereby increased receptor activity leads to decreased CNP production and vice versa. NPR2-mediated cGMP production in response to CNP was markedly increased in the proband's skin fibroblasts, suggesting that the responsiveness of the mutant NPR2 expressed in the bone and many other tissues of the proband is also enhanced. Nevertheless, plasma cGMP concentrations were normal. However, in our experience even very high plasma levels of active CNP, achieved by intravenous infusion of synthetic peptide, have little if any effect on plasma cGMP levels in healthy controls [35]. Compared with cGMP increments evoked by equimolar concentrations of ANP and BNP, those induced by CNP were less than 10%. Other studies showed that plasma cGMP is mainly derived from vascular endothelial cells, which express high levels of NPR1 (the ANP receptor) but very low levels of NPR2 [36]. Hence, it is not surprising that plasma cGMP concentrations were normal in the proband.

The tall stature (height +5.2 SDS) is more severe in this case compared to the reported cases in the Japanese family with an activating mutation within the GC domain of NPR2 (height +2.7 to +3.8 SDS) [11], especially considering the fact that the proband would have been even taller without epiphysiodesis (his arm span of 232 cm suggests that without intervention adult height would have been approximately 230 cm). Of note, excessive length was already evident at birth. Other features, however, like a Marfanoid phenotype and skeletal deformities were much less pronounced than in the Japanese patients and in patients with CNP overproduction [9-11]. What causes this difference in phenotype is currently unclear; it might be related to the location of the mutation within the NPR2 (KHD versus GC domain) or perhaps to the different genetic background. Importantly, the findings in the proband imply that an activating *NPR2* mutation should be considered as a possible cause of isolated tall stature without dysmorphic features or skeletal deformities and could be screened for by measuring NTproCNP, provided renal function is normal.

How does the heterozygous Arg655Cys substitution within the conserved region of the KHD enhance NPR2 activity? As mentioned above, the function of this domain is not well understood. Although being inactive with respect to phosphorylating substrates [30], it binds ATP and modulates the enzymatic activity of the distal GC domain [37]. Furthermore, several studies showed that in the absence of ligand the KHD represses the activity of the GC domain [2, 30]. NPR activation possibly follows a ligand-induced rearrangement mechanism [38] and ATP binding to the KHD seems to allosterically modulate the ligand-stimulated catalytic activity of the GC domain [29, 37].

As illustrated in Figures 5B and C, homology modeling of the KHD suggests that Arg655 is solvent-exposed and does not affect ATP binding. For these modeling studies we used

different kinase structure templates, some of which form dimeric assemblies in the crystal. Sequence comparisons indicated that the KHD of NPR2 showed the highest homology (33% identity, 51% similarity on amino acid sequence level) to the serine/threonine kinase Ctr1 (constitutive triple response 1 kinase), which is a member of the raf-like kinases [22]. In the crystal structure Ctr1 has a dimeric assembly with a rather large interface between the two kinase subunits. An identical dimer architecture is also seen in crystal structures of the Raf-kinases C-Raf and B-Raf indicating that the dimer arrangement is of functional relevance. The monomeric model of the NPR2 KHD could be docked onto this dimer arrangement forming a similar large interface (see Figure 5). In our dimer model of the KHD of NPR2, Arg655 is located close to the dimer interface with the Cα atoms of Arg655 in either subunit distanced by about 6 Å only. Thus, the exchange of this arginine by a cysteine could bring the two thiol groups of a homodimeric mutant NPR2 in close proximity allowing formation of an intermolecular disulfide bond, thereby possibly leading to a semiactivated state of NPR2. Although disulfide bond formation inside the cytoplasm is rare, a recent study using a fluorescence resonance energy transfer (FRET)-based thiol-containing sensor showed that despite the reducing environment a significant amount of the sensor contained disulfide bonds [39]. Alternatively, the close proximity of Arg655 to the dimer interface could point to a mechanism relying on a relief from steric/electrostatic repulsion. Substitution of the bulky and positively charged arginine by a small and neutral cysteine might favor or ease the conformational rearrangement induced by extracellular CNP binding and facilitate the allosteric activation by intracellular ATP. This hypothesis is supported by our observation that the stimulatory effect of ATP on CNP-dependent guanylate cyclase activity of the mutant NPR2 was markedly enhanced.

Besides stimulating skeletal growth, CNP/NPR2 signalling is involved in the modulation of cardiovascular, neuronal and reproductive functions [40]. It is therefore important to mention that the proband has several medical problems outside the skeleton. In particular he has gynaecomastia and 24 h prolactin secretion was increased, which could not be attributed to medication. Increased prolactin secretion might be related to the activating *NPR2* mutation, as CNP injected into the third ventricle of castrated male rats and ovariectomised female rats increased plasma prolactin [41]. CNP does not seem to act directly on lactotrophs but may act at the hypothalamic level, where both CNP and NPR2 are expressed [42]. In fact, CNP and NTproCNP are present in human cerebrospinal fluid at levels that greatly exceed those in plasma [43].

In addition, the proband has a polyneuropathy which was attributed to diabetes mellitus but was diagnosed more than 10 years before diabetes mellitus was apparent. It is interesting to speculate on a role of the *NPR2* mutation because NPR2 was shown to be essential for sensory axon bifurcation in the spinal cord of mice [6] and CNP knockout mice

display a decreased response to pain [44]. In addition, the foot ulcers in the proband were regarded to be secondary to the diabetes and venous insufficiency, but again it is tempting to speculate on a direct effect of altered NPR2 function, since NPR2 has been suggested to play a role in wound healing [45].

Lastly, CNP, via NPR2, was reported to counteract experimental hypertensive cardiac remodeling and to inhibit valve interstitial cell differentiation [46, 47]. Tricuspid and mitral valve pathologies were reported in a 14 yr old girl with CNP overexpression [9]. However, the proband did not exhibit changes in cardiac size or function, with exception of atrial fibrillation.

It is unclear whether the heterozygous microdeletion on chromosome 15 found in the proband has any clinical consequences. Two of the proteins affected by this deletion have been studied in genetic mouse models. The *Pde8a* knockout mouse did not show an obvious change in body size or bone length (personal communication of Prof. Beavo), neither did the alpha-kinase 2 knockout mouse [48]. In humans, a homozygous mutation in *ZNF592* causes CAMOS (cerebellar ataxia with mental retardation, optic atrophy and skin abnormalities) and proportionate short stature [49]. Overall, these data suggest that haploinsufficiency of the genes affected by the heterozygous microdeletion on chromosome 15 does not contribute to the tall stature of the proband.

In conclusion, we report a novel activating *NPR2* mutation located in the KHD, which results in extremely tall stature without a Marfanoid phenotype or severe skeletal abnormalities. This activating mutation indicates that the KHD, whose function is still poorly understood, is crucially involved in regulating guanylate cyclase activity of NPR2. Whether the hyperprolactinemia, diabetes mellitus and polyneuropathy of the proband are also related to the *NPR2* mutation or to the microdeletion on chromosome 15, awaits further investigation.

Acknowledgements

We are grateful to Prof. Beavo for his advice on PDE8a function. We thank Mila Jhamai and Pascal Arp for technical work concerning exome sequencing and Robert Kraaij, Jeroen van Rooij, Stephan Nouwens and Marijn Verkerk for bioinformatics and ICT support. We thank the patient for his willingness to undergo the various tests. MKs work was supported by the DFG (SFB 688 and KU1037/5-1) and WO received grant support from Novo Nordisk.

chapter
8

Reference List

1. Potter LR (2011) Guanylyl cyclase structure, function and regulation. Cell Signal 23 (12):1921-1926

2. Tremblay J, Desjardins R, Hum D, Gutkowska J, and Hamet P (2002) Biochemistry and physiology of the natriuretic peptide receptor guanylyl cyclases. Mol Cell Biochem 230 (1-2):31-47

3. Misono KS, Philo JS, Arakawa T, Ogata CM, Qiu Y, Ogawa H, and Young HS (2011) Structure, signaling mechanism and regulation of the natriuretic peptide receptor guanylate cyclase. FEBS J 278 (11):1818-1829

4. Yasoda A, Ogawa Y, Suda M, Tamura N, Mori K, Sakuma Y, Chusho H, Shiota K, Tanaka K, and Nakao K (1998) Natriuretic peptide regulation of endochondral ossification. Evidence for possible roles of the C-type natriuretic peptide/guanylyl cyclase-B pathway. J Biol Chem 273 (19):11695-11700

5. Zhang M, Su YQ, Sugiura K, Xia G, and Eppig JJ (2010) Granulosa cell ligand NPPC and its receptor NPR2 maintain meiotic arrest in mouse oocytes. Science 330 (6002):366-369

6. Schmidt H, Stonkute A, Juttner R, Schaffer S, Buttgereit J, Feil R, Hofmann F, and Rathjen FG (2007) The receptor guanylyl cyclase Npr2 is essential for sensory axon bifurcation within the spinal cord. J Cell Biol 179 (2):331-340

7. Bartels CF, Bukulmez H, Padayatti P, Rhee DK, van Ravenswaaij-Arts C, Pauli RM, Mundlos S, Chitayat D, Shih LY, Al-Gazali LI, Kant S, Cole T, Morton J, Cormier-Daire V, Faivre L, Lees M, Kirk J, Mortier GR, Leroy J, Zabel B, Kim CA, Crow Y, Braverman NE, van den Akker F, and Warman ML (2004) Mutations in the transmembrane natriuretic peptide receptor NPR-B impair skeletal growth and cause acromesomelic dysplasia, type Maroteaux. Am J Hum Genet 75 (1):27-34

8. Olney RC, Bukulmez H, Bartels CF, Prickett TC, Espiner EA, Potter LR, and Warman ML (2006) Heterozygous mutations in natriuretic peptide receptor-B (NPR2) are associated with short stature. J Clin Endocrinol Metab 91 (4):1229-1232

9. Bocciardi R, Giorda R, Buttgereit J, Gimelli S, Divizia MT, Beri S, Garofalo S, Tavella S, Lerone

M, Zuffardi O, Bader M, Ravazzolo R, and Gimelli G (2007) Overexpression of the C-type natriuretic peptide (CNP) is associated with overgrowth and bone anomalies in an individual with balanced t(2;7) translocation. Hum Mutat 28 (7):724-731

10. Moncla A, Missirian C, Cacciagli P, Balzamo E, Legeai-Mallet L, Jouve JL, Chabrol B, Le MM, Plessis G, Villard L, and Philip N (2007) A cluster of translocation breakpoints in 2q37 is associated with overexpression of NPPC in patients with a similar overgrowth phenotype. Hum Mutat 28 (12):1183-1188

11. Miura K, Namba N, Fujiwara M, Ohata Y, Ishida H, Kitaoka T, Kubota T, Hirai H, Higuchi C, Tsumaki N, Yoshikawa H, Sakai N, Michigami T, and Ozono K (2012) An overgrowth disorder associated with excessive production of cGMP due to a gain-of-function mutation of the natriuretic peptide receptor 2 gene. PLoS One 7 (8):e42180

12. Veldhuis JD, Erickson D, Wigham J, Weist S, Miles JM, and Bowers CY (2011) Gender, sex-steroid, and secretagogue-selective recovery from growth hormone-induced feedback in older women and men. J Clin Endocrinol Metab 96 (8):2540-2547

13. Roelfsema F, Pijl H, Keenan DM, and Veldhuis JD (2012) Prolactin secretion in healthy adults is determined by gender, age and body mass index. PLoS One 7 (2):e31305

14. Roelfsema F, Biermasz NR, Veldman RG, Veldhuis JD, Frolich M, Stokvis-Brantsma WH, and Wit JM (2001) Growth hormone (GH) secretion in patients with an inactivating defect of the GH-releasing hormone (GHRH) receptor is pulsatile: evidence for a role for non-GHRH inputs into the generation of GH pulses. J Clin Endocrinol Metab 86 (6):2459-2464

15. Liu PY, Keenan DM, Kok P, Padmanabhan V, O'Byrne KT, and Veldhuis JD (2009) Sensitivity and specificity of pulse detection using a new deconvolution method. Am J Physiol Endocrinol Metab 297 (2):E538-E544

16. Keenan DM, Roelfsema F, Biermasz N, and Veldhuis JD (2003) Physiological control of pituitary hormone secretory-burst mass, frequency, and waveform: a statistical formulation and analysis. Am J Physiol Regul Integr Comp Physiol 285 (3):R664-R673

17. Santen GW, Aten E, Sun Y, Almomani R, Gilissen C, Nielsen M, Kant SG, Snoeck IN, Peeters EA, Hilhorst-Hofstee Y, Wessels MW, den Hollander NS, Ruivenkamp CA, van Ommen GJ, Breuning MH, den Dunnen JT, van HA, and Kriek M (2012) Mutations in SWI/SNF chromatin

remodeling complex gene ARID1B cause Coffin-Siris syndrome. Nat Genet 44 (4):379-380

18. Chao YC, Cheng CJ, Hsieh HT, Lin CC, Chen CC, and Yang RB (2010) Guanylate cyclase-G, expressed in the Grueneberg ganglion olfactory subsystem, is activated by bicarbonate. Biochem J 432 (2):267-273

19. Schroter J, Zahedi RP, Hartmann M, Gassner B, Gazinski A, Waschke J, Sickmann A, and Kuhn M (2010) Homologous desensitization of guanylyl cyclase A, the receptor for atrial natriuretic peptide, is associated with a complex phosphorylation pattern. FEBS J 277 (11):2440-2453

20. Klaiber M, Dankworth B, Kruse M, Hartmann M, Nikolaev VO, Yang RB, Volker K, Gassner B, Oberwinkler H, Feil R, Freichel M, Groschner K, Skryabin BV, Frantz S, Birnbaumer L, Pongs O, and Kuhn M (2011) A cardiac pathway of cyclic GMP-independent signaling of guanylyl cyclase A, the receptor for atrial natriuretic peptide. Proc Natl Acad Sci U S A 108 (45):18500-18505

21. Kamp GA, Ouwens DM, Hoogerbrugge CM, Zwinderman AH, Maassen JA, and Wit JM (2002) Skin fibroblasts of children with idiopathic short stature show an increased mitogenic response to IGF-I and secrete more IGFBP-3. Clin Endocrinol (Oxf) 56 (4):439-447

22. Mayerhofer H, Panneerselvam S, and Mueller-Dieckmann J (2012) Protein kinase domain of CTR1 from Arabidopsis thaliana promotes ethylene receptor cross talk. J Mol Biol 415 (4):768-779

23. Brown K, Vial SC, Dedi N, Long JM, Dunster NJ, and Cheetham GM (2005) Structural basis for the interaction of TAK1 kinase with its activating protein TAB1. J Mol Biol 354 (5):1013-1020

24. Lowe ED, Noble ME, Skamnaki VT, Oikonomakos NG, Owen DJ, and Johnson LN (1997) The crystal structure of a phosphorylase kinase peptide substrate complex: kinase substrate recognition. EMBO J 16 (22):6646-6658

25. Arnold K, Bordoli L, Kopp J, and Schwede T (2006) The SWISS-MODEL workspace: a web-based environment for protein structure homology modelling. Bioinformatics 22 (2):195-201

26. Florkowski CM, Richards AM, Espiner EA, Yandle TG, and Frampton C (1994) Renal, endocrine, and hemodynamic interactions of atrial and brain natriuretic peptides in normal men. Am J Physiol 266 (4 Pt 2):R1244-R1250

27. Olney RC, Permuy JW, Prickett TC, Han JC, and Espiner EA (2012) Amino-terminal propeptide of C-type natriuretic peptide (NTproCNP) predicts height velocity in healthy children. Clin Endocrinol (Oxf) 77 (3):416-422

28. Beis I and Newsholme EA (1975) The contents of adenine nucleotides, phosphagens and some glycolytic intermediates in resting muscles from vertebrates and invertebrates. Biochem J 152 (1):23-32

29. Duda T, Yadav P, and Sharma RK (2011) Allosteric modification, the primary ATP activation mechanism of atrial natriuretic factor receptor guanylate cyclase. Biochemistry 50 (7):1213-1225

30. Potter LR and Hunter T (1998) Identification and characterization of the major phosphorylation sites of the B-type natriuretic peptide receptor. J Biol Chem 273 (25):15533-15539

31. Duda T, Yadav P, Jankowska A, Venkataraman V, and Sharma RK (2000) Three dimensional atomic model and experimental validation for the ATP-Regulated Module (ARM) of the atrial natriuretic factor receptor guanylate cyclase. Mol Cell Biochem 214 (1-2):7-14

32. Schwartz PA and Murray BW (2011) Protein kinase biochemistry and drug discovery. Bioorg Chem 39 (5-6):192-210

33. Prickett TC, Lynn AM, Barrell GK, Darlow BA, Cameron VA, Espiner EA, Richards AM, and Yandle TG (2005) Amino-terminal proCNP: a putative marker of cartilage activity in postnatal growth. Pediatr Res 58 (2):334-340

34. Prickett T, Olney R, Cameron V, Ellis M, Richards A, and Espiner E (2012) Impact of Age, Phenotype and Cardio-Renal Function on Plasma C-Type and B-Type Natriuretic Peptide Forms in an Adult Population. Clin Endocrinol (Oxf)

35. Hunt PJ, Richards AM, Espiner EA, Nicholls MG, and Yandle TG (1994) Bioactivity and metabolism of C-type natriuretic peptide in normal man. J Clin Endocrinol Metab 78 (6):1428-1435

36. Stasch JP, Kazda S, and Neuser D (1989) Different effects of ANP and nitroprusside on cyclic GMP extrusion of isolated aorta. Eur J Pharmacol 174 (2-3):279-282

37. Duda T, Yadav P, Jankowska A, Venkataraman V, and Sharma RK (2001) Three dimensional atomic model and experimental validation for the ATP-Regulated Module (ARM) of the atrial natriuretic factor receptor guanylate cyclase. Mol Cell Biochem 217 (1-2):165-172

38. Ogawa H, Qiu Y, Ogata CM, and Misono KS (2004) Crystal structure of hormone-bound atrial natriuretic peptide receptor extracellular domain: rotation mechanism for transmembrane signal transduction. J Biol Chem 279 (27):28625-28631

39. Ostergaard H, Tachibana C, and Winther JR (2004) Monitoring disulfide bond formation in the eukaryotic cytosol. J Cell Biol 166 (3):337-345

40. Kuhn M (2009) Function and dysfunction of mammalian membrane guanylyl cyclase receptors: lessons from genetic mouse models and implications for human diseases. Handb Exp Pharmacol (191):47-69

41. Huang FL, Skala KD, and Samson WK (1992) C-type natriuretic Peptide stimulates prolactin secretion by a hypothalamic site of action. J Neuroendocrinol 4 (5):593-597

42. Jankowski M, Reis AM, Wang D, and Gutkowska J (2004) Postnatal ontogeny of natriuretic peptide systems in the rat hypothalamus. Brain Res Dev Brain Res 152 (1):39-46

43. Schouten BJ, Prickett TC, Hooper AA, Hooper GJ, Yandle TG, Richards AM, and Espiner EA (2011) Central and peripheral forms of C-type natriuretic peptide (CNP): evidence for differential regulation in plasma and cerebrospinal fluid. Peptides 32 (4):797-804

44. Kishimoto I, Tokudome T, Horio T, Soeki T, Chusho H, Nakao K, and Kangawa K (2008) C-type natriuretic peptide is a Schwann cell-derived factor for development and function of sensory neurones. J Neuroendocrinol 20 (11):1213-1223

45. Abbey-Hosch SE, Cody AN, and Potter LR (2004) Sphingosine-1-phosphate inhibits C-type natriuretic peptide activation of guanylyl cyclase B (GC-B/NPR-B). Hypertension 43 (5):1103-1109

46. Soeki T, Kishimoto I, Okumura H, Tokudome T, Horio T, Mori K, and Kangawa K (2005) C-type natriuretic peptide, a novel antifibrotic and antihypertrophic agent, prevents cardiac remodeling after myocardial infarction. J Am Coll Cardiol 45 (4):608-616

47. Yip CY, Blaser MC, Mirzaei Z, Zhong X, and Simmons CA (2011) Inhibition of pathological differentiation of valvular interstitial cells by C-type natriuretic peptide. Arterioscler Thromb Vasc Biol 31 (8):1881-1889

48. Van S, I, Ding ZM, Shi ZZ, Read RW, Hansen G, and Vogel P (2012) Cardiomyopathy in alpha-Kinase 3 (ALPK3)-Deficient Mice. Vet Pathol 49 (1):131-141

49. Nicolas E, Poitelon Y, Chouery E, Salem N, Levy N, Megarbane A, and Delague V (2010) CAMOS, a nonprogressive, autosomal recessive, congenital cerebellar ataxia, is caused by a mutant zinc-finger protein, ZNF592. Eur J Hum Genet 18 (10):1107-1113

Supplemental Figure + Table

A

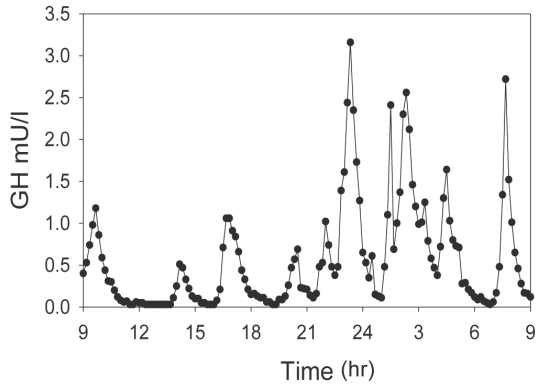

B

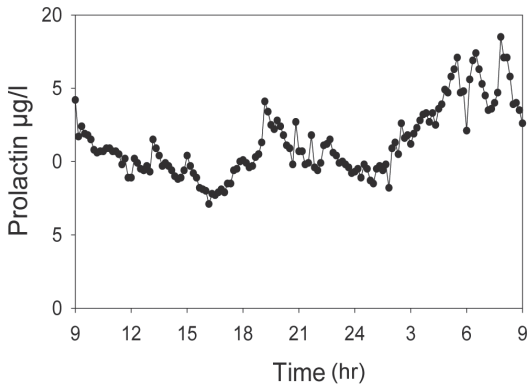

Supplemental figure 1 Profiles (24 h) of growth hormone and prolactin secretion.
(A) Pulsatile GH secretion of the proband. Compared to healthy controls of similar age GH secretion is low, consistent with his increased BMI. For details of the secretion see supplemental table 1.
(B) Prolactin secretion was clearly elevated (see supplemental table 1).

Table 1 Deconvolution analysis of 24 h serum hormone profiles in controls and proband

	GH secretion in controls	Patient	PRL secretion in controls	Patient
Pulse frequency (no/24 h)	13 (10-21)	14	20 (16-24)	19
Half-life (min)	14.3 (8-25)	17.7	32 (20-42)	23.8
Pulse mode day (min)	14.2 (4.6-30)	13.9	12.1 (6.4-24)	3.79
Pulse mode night (min)	16.7 (6.9-30)	16.5	5.3 (3-14.6)	5.14
Basal secretion (units/liter)	4.2 (1.5 -42)	3.8	83 (44-201)	491
Pulsatile secretion (units/liter)	72 (27-277)	40.3	83 (30-125)	188
Total secretion (units/liter)	73 (32-319)	44.1	183 (99-325)	679
Pulse regularity (unitless)	1.40 (1.13-1.70)	1.28	1.99 (1.41-2.80)	2

Data are median and range. GH is expressed in mU/liter and prolactin as µg/liter.
Secretion rates are in unit/liter distribution volume per 24 h.